where four particles, two counterions and two polyions, are close together. This situation, which is unphysical in our case, is included in the hypernetted chain equation (see Figure 11 of ref 25), while, in fact, it may be largely canceled by the next bridge graph, as explained previously.[25,40,41] Even without doing the elaborate calculation, one can see that the contribution of this graph will extend beyond the distance $2(r_p{}^* + r_c{}^*)$, where $r_p{}^*$ and $r_c{}^*$ are the radii of the polyion and coion. This is consistent with the results of 2:2 electrolytes[40] and with our computer results for the counterion–counterion correlation function. These "collective interactions" between a polyion and several counterions may also explain why the "nearly universal" behavior of the bridge function seems to break down in this case. Because the counterions interact mainly on the surface of the polyion, and at the same time avoid contact with each other, there seems little reason to expect a faithful hard-sphere model bridge function for the counterion–counterion interaction in the usual range of packing fractions.

Nevertheless, we have attempted to improve the HNC calculation with a model, hard-sphere bridge function chosen empirically. Since the counterion–counterion correlation function is in most serious disagreement with the computer simulation, we have chosen to apply the corrections to this one function. In accordance with our computer simulations, we have chosen the reference hard-sphere diameter for the bridge function model to be $2(r_p{}^* + r_c{}^*) = 4.4$ nm. This is the range in which the counterion–counterion correlation function is affected by the presence of a polyion. With a choice of the reduced density of the reference hard-sphere liquid $\rho^* = 0.125$, we obtain the agreement displayed in Figure 7. It is interesting that a correction to $g_{cc}(r)$ also corrects $g_{pc}(r)$, while the improvement to $g_{pp}(r)$ is less significant and is not shown here. This example is designed to show only that a

more serious study, similar to our electrolyte work,[29,41] is likely to yield a measurable improvement over the hypernetted chain approximation.

4. Conclusions

The comparison between the Monte Carlo simulations and the hypernetted chain integral equation indicates that HNC approximation is useful for asymmetric electrolytes in the range of parameters examined here. However, since its thermodynamic predictions are intrinsically inconsistent, it yields different results for the virial and the compressibility pressure. The essential defect is that the HNC theory overestimates the concentration of counterions close to the polyion, and moreover it substantially overestimates $g_{cc}(r)$ in a wide range of distances. This leads to an underestimate of the degree of structure in the solution. The position of the first peak in the polyion–polyion correlation function is at too short a distance, and its magnitude is too small. This fact should be considered when intermicellar structure factors, obtained from small-angle neutron scattering, are analyzed using the hypernetted chain equation. In addition, the HNC equation erroneously predicts spinodal decomposition in the region of complete mixing. The hypernetted chain approximation may be useful for studying the catalytic effect of the micelles on certain chemical reactions, where a substantial improvement over the traditional meanfield approach is needed.

Ab Initio Study of Destabilized π-Conjugated Systems with Large π-Overlap: Sulfur Trimethylene and Chlorine Trimethylene Cation. Electrostatics as a Dominant Factor in Multiple Bonding for Second-Row Elements

Andrzej Rajca*,[1] and Kee Hag Lee[2]

Contribution from the Department of Chemistry, University of California, Berkeley, California 94720. Received July 28, 1988

Abstract: Ab initio calculations at the MP2/6-31G**//HF/6-31G*/ZPVE level of theory indicate that conjugative stabilization in 6π-electron Y-conjugated systems, $X(CH_2)_3$ and XO_3 (X = P (anion), S (neutral), and Cl (cation)), is dominated by electrostatic interactions; that is, increasing the X–C overlap and decreasing X–C charge separation via change in electronegativity of X *decreases* stability of the D_{3h}-symmetric structures versus the structures with lower symmetry (less π-overlap). These energy patterns are reflected in properties of the electron densities (ellipticities at bond critical points, integrated atomic populations, etc.) at the HF/6-31G* level for the D_3- and D_{3h}-symmetric structures; the more the atomic charges (relative electronegativities) approach or even exceed the formal charges of "no formal double bond" resonance structure, $X^{n+}(Z^-)_3$, the greater is the preference for the geometries where π-conjugation is feasible. $S(CH_2)_3$ (D_3), which is most predisposed to π-overlap, shows signs of a very weak bonding; it possesses a "pseudoatom" (local maximum of the electron density) and two bond critical points along each SC bond axis. For the ylide $S(CH_2)_3$, a double-well potential energy surface (PES) is found with two D_3-symmetric local minima that are 9 kcal mol⁻¹ below the D_{3h}-symmetric transition structure for methylene rotation; 47 kcal mol⁻¹ below the D_3-symmetric structure, a very flat fragment of the PES, which corresponds to the methylene thirane structure, is located. Preparation of the Y-conjugated $S(CH_2)_3$ (D_3) may be quite difficult but feasible in view of the fact that the barrier for its collapse to the global minimum is estimated as close to 6.0 kcal mol⁻¹ (MP3/6-31G*//HF/6-31G*/ZPVE); IR and Raman spectra calculated at the HF/6-31G* level may aid the experiment.

Recent years have witnessed proliferation of multiple-bonded molecules containing elements beyond the first row.[3] Such

molecules are generally quite unstable and, therefore, isolated either in a matrix or stabilized by sterically bulky substituents. Both experimental and theoretical works are predominantly confined to systems with just one multiple bond.[4] The next logical

(3) Recent examples. C=Sn: Berndt, A. *Angew. Chem., Int. Ed. Engl.* **1987**, *26*, 546. C=Ge: Couret, C.; Escudie, J.; Satge, J.; Lazraq, M. *J. Am. Chem. Soc.* **1987**, *109*, 4411.

$S(CH_2)_3$ and $Cl(CH_2)_3{}^+$ π-Conjugated Systems

J. Am. Chem. Soc., Vol. 111, No. 12, 1989 4167
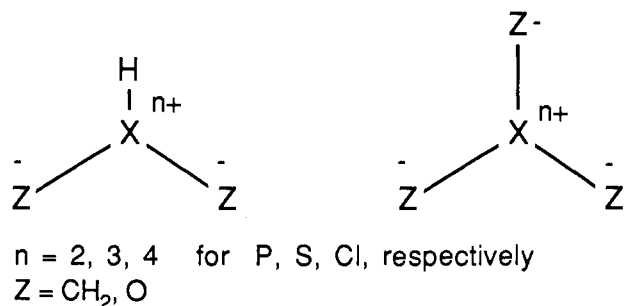

n = 2, 3, 4   for P, S, Cl, respectively
Z = CH₂, O

Figure 1. Resonance structures ("no formal double bond") for the 4π- and 6π-electron allyl and Y-conjugated system, respectively.

step is investigation of conjugated systems.

Allyl, which is the simplest conjugated system, has been theoretically examined in depth for first-row elements. It appears that for π-conjugated molecules containing elements with different electronegativities, such as ester, amide,[5] nitrous acid,[6] or carboxylate ion,[7] not π-overlap but rather polarization effects are most important. Introduction of a second-row element at the central site of allyl, e.g., 2-silallyl ion ($H_2CSiHCH_2$ cation or anion), even leads to the observation that increased π-overlap (and decreased polarization effects) in the cation versus anion is detrimental to the stability of the cation's lowest singlet state.[8] If the electrostatic interactions in 4π-electron allyls, XZ_2, are indeed dominant, they should be even more pronounced in 6π-electron Y-conjugated systems,[9] XZ_3 (X = P (anion), S (neutral), Cl (cation); Z = oxo, CH_2, NH) for the following reasons: (i) three (instead of two) terminal charges or multipoles can electrostatcally interact with one charge or multipole at the "X" (Figure 1); (ii) π-overlap in the Y-conjugated systems is expected to be less compared with the allylic counterparts as suggested by the Hückel bond orders of 0.58 and 0.71, respectively.[10] More qualitatively, both the Y-conjugated and allyl system possess only one bonding π-MO that is delocalized over four and three centers, respectively. Thus, the relative stabilities of similar π-conjugated molecules should be determined by relative contributions of the resonance structure without formal double bonds (Figure 1).

Consequently, an increase in electronegativity of "X", so as to match or exceed the electronegativity of "Z" in XZ_3, will be destabilizing or stabilizing if the electrostatics or the π-overlap, respectively, is important. 6π-Electron Y-conjugated systems are selected with "X" = P, S, and Cl and "Z" = oxo, amido, and methylene. The following parent systems or derivatives are known: $PO_3{}^-$, $P(NH)_3{}^-$, SO_3, $S(NH)_3$, and most recently, $P(CH_2)_3{}^-$, in addition to a few variations with nonequivalent "Z", e.g., $HNSO_2$, H_2CSO_2, $H_2CS(O)NH$, etc.[11] Notably, systems were electro-

Table I. Relative Energies (kcal mol⁻¹) for Structures with Fully Optimized Geometries within the Indicated Point Group of Symmetry Constraints

		D_3	D_{3h}	C_{2v}	C_{3v}	C_s	C_{s^2}
1	3-21+G*ᵃ	0.0	1.0	13.4	62.4	4.4	
	6-31+G*ᵃ	0.0				-12.1	
2	3-21G(*)	0.0	6.6	16.0	30.0	-46.7	28.8
	6-31G*	0.0	6.4		26.8	-55.2	25.0
	MP2/6-31G**ᵇ	0.0	11.4		0.5	-47.7	
	MP2/6-31G*	0.0			0.5		
	MP3/6-31G*	0.0			7.7		
3	3-21G(*)	0.0	24.5	23.4	-2.0	-92.2	
	6-31G*	0.0	23.7		-2.6		

ᵃReferences 14 and 27. ᵇThe HF/6-31G* optimized geometry is used for all MP calculations.

Table II. Imaginary and Important Real Harmonic Vibrational Frequencies (cm⁻¹) and Zero-Point Vibrational Energies (ZPVE, kcal mol⁻¹) at the RHF/6-31G* Level

	ZPVE	frequency		normal mode
2-D_3	51.99	A_2	281.1	pyramidalization at S ($D_3 \rightarrow C_{3v}$)
		A_1	522.2	CH_2 conrotatory twist ($D_3 \rightarrow D_{3h}$)
2-D_{3h}	50.00	A_1''	i467.5	CH_2 conrotatory twist ($D_{3h} \rightarrow D_3$)
		A_2''	204.5	pyramidalization at S and C
2-C_{3v}	50.33	E	i293.9	ring closure ($C_{3v} \rightarrow C_s$)
2-C_s	53.07	A''	i361.5	pyramidalization of the *exo* CH_2 ($C_s \rightarrow C_1$)
2-C_{s^2}	50.99	A''	i630.9	ring closure ($C_s \rightarrow C_1$)
2-D_3	51.63	A_2	85.2	pyramidalization at Cl ($D_3 \rightarrow C_{3v}$)
		A_1	464.4	CH_2 conrotatory twist ($D_3 \rightarrow D_{3h}$)

negativity of "X" approaches or exceeds "Z" are not yet experimentally realized, e.g., $S(CH_2)_3$ and $ClZ_3{}^+$ (Z = O, NH, CH_2).[12] Our results reveal novel aspects of this problem and point to Y-conjugated $S(CH_2)_3$ as a borderline case in π-bonding; information that may be helpful in isolation of $S(CH_2)_3$ or its derivatives is provided.

Calculational Methods

All calculations were carried out for the lowest singlet states with full geometry optimization at the restricted Hartree–Fock (HF) level using the 3-21G(*) basis set that includes a single set of polarization functions at chlorine or sulfur; 3-21+G* basis set results for P-containing anions are described elsewhere.[14] Geometries for the selected structures were reoptimized and harmonic vibrational frequencies were calculated using the 6-31G* basis set (6-31+G* for anions). Analytical second derivatives were employed. Frequency calculations on 3-D_3, which possesses one real frequency below 100 cm⁻¹, were performed using optimized geometry with maximum Cartesian force of less than 3.1 × 10⁻⁶ hartree bohr⁻¹. The 6-31G* geometries were used for single point calculations using second-order Møller–Plesset (MP2) perturbation theory with 6-31G** basis set (polarization functions at all atoms). Standard 6-311G** and 6-31G(2d,p) basis sets stored in GAUSSIAN 86 were also employed for single point calculations. GAUSSIAN 82[15] and GAUSSIAN 86[16] programs were used for all calculations described in this paragraph.

One method for the examination of electron densities involves basis set populations such as Reed and Weinhold's[17] natural populations (NP). Natural atomic orbital (NAO) populations for the π system were also examined.[17] The other method is based on topological analysis of the electron density in the real, three-dimensional coordinate, space (3-D) and performed using the approach of Bader.[18] Bond critical points, that

(4) Schleyer, P. v. R.; Kost, D. *J. Am. Chem. Soc.* **1988**, *110*, 2105. Schmidt, M. W.; Truong, P. N.; Gordon, M. S. *J. Am. Chem. Soc.* **1987**, *109*, 5217. Truong, T. N.; Gordon, M. S. *J. Am. Chem. Soc.* **1986**, *108*, 1775. Lee, J.-G.; Boggs, J. E.; Cowley, A. H. *J. Chem. Soc., Chem. Commun.* **1985**, 773. Kudo, T.; Nagase, S. *Organometallics* **1986**, *5*, 1207. Dobbs, K. D.; Hehre, W. *Organometallics* **1986**, *5*, 2057. Lahr, L. C.; Schlegel, H. B.; Morokuma, K. *J. Phys. Chem.* **1984**, *88*, 1981. Lohr, L. L.; Panos, S. H. *J. Phys. Chem.* **1984**, *88*, 2992. Cook, C. M.; Allen, L. C. *Organometallics* **1982**, *1*, 246.

(5) Wiberg, K. B.; Laidig, K. E. *J. Am. Chem. Soc.* **1987**, *109*, 5935.

(6) Wiberg, K. B. *J. Am. Soc. Chem.*, in press. Thomas, T. D. *J. Am. Chem. Soc.*, in press.

(7) Siggel, M. R.; Thomas, T. D. *J. Am. Chem. Soc.* **1986**, *108*, 4360. Siggel, M. R.; Streitwieser, A., Jr.; Thomas, T. D. *J. Am. Chem. Soc.* **1988**, *110*, 8022.

(8) Rajca, A.; Streitwieser, A., Jr. *Organometallics* **1988**, *7*, 2215.

(9) Examples of the Y-conjugated systems are $PO_3{}^-$, $CO_3{}^{2-}$, SO_3. Derivatives of the prototype all-carbon system, trimethylenemethane dianion, possess such a remarkable thermodynamic stability that the term "Y-aromaticity" has been invoked. See: (a) Finnegan, R. A. *Ann. N.Y. Acad. Sci.* **1969**, *152*, 242. Gund, P. J. *J. Chem. Educ.* **1972**, *49*, 100. (b) Rajca, A.; Tolbert, L. M. *J. Am. Chem. Soc.* **1988**, *110*, 871.

(10) Lowe, J. P. *Quantum Chemistry*; Academic Press: New York, 1978.

(11) Friedman, J. M.; Freeman, S.; Knowles, J. R. *J. Am. Chem. Soc.* **1988**, *110*, 1268 and references therein. Appel, R.; Gaitzsch, E.; Knoch, F. *Angew. Chem., Int. Ed. Engl.* **1985**, *24*, 589. Lerch, C.; Niemann, J.; Schoeller, W. W. *Phosphorus Sulfur* **1987**, *30*, 503. For organosulfur compounds, see: *Methoden der organischen Chemie* (Houben-Weyl), Klaman, D., Ed.; 1985; Vol. E11.

(12) The referee has pointed out that the group electronegativities can be used.

(13) Hehre, W. J.; Radom, L.; Schleyer, P. v. R.; Pople, J. A. *Ab Initio Molecular Orbital Theory*; Wiley: New York, 1986.

(14) Rajca, A.; Rice, J. E.; Streitwieser, A., Jr.; Schaefer, H. F. III *J. Am. Chem. Soc.* **1987**, *109*, 4189.

(15) Binkley, J. S.; Frish, M. J.; DeFrees, D. J.; Raghavachari, K.; Whiteside, R. A.; Schlegel, H. B.; Fluder, E. M.; Pople, J. A. GAUSSIAN 82; Carnegie-Mellon University: Pittsburgh, PA.

(16) Frish, M. J.; Binkley, J. S.; Schlegel, H. B.; Raghavachari, K.; Melius, C. F.; Martin, R. L.; Stewart, J. J. P.; Bobrowicz, F. W.; Rohlfing, C. M.; Kahn, L. R.; Defrees, D. J.; Seeger, R.; Whiteside, R. A.; Fox, D. J.; Fleuder, E. M.; Pople, J. A. GAUSSIAN 86; Carnegie-Mellon Quantum Chemistry Publishing Unit, Pittsburgh, PA, 1984.

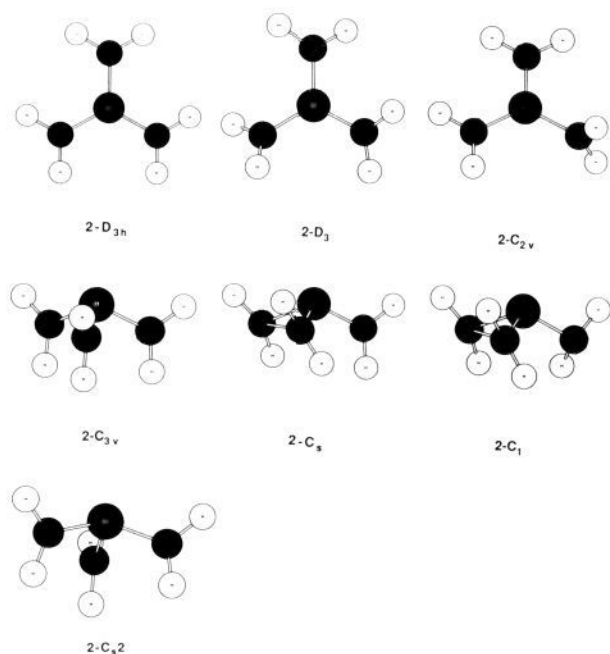(17) Reed, A. E.; Weinhold, F. *J. Am. Chem. Soc.* **1985**, *107*, 1919.

Figure 2. Structures of sulfur trimethylene, $S(CH_2)_3$ (**2**).

is, zero-gradient points in 3-D that possess two negative curvatures and one positive curvature of the electron density in 3-D, were located using the program EXTREME.[18] Zero-flux surfaces are found for the atoms and the electron density inside them was integrated with PROAIMS.[18]

Results and Discussion

$S(CH_2)_3$ (**2**) **Potential Energy Surface (PES).** Geometries for all structures of **2** are initially optimized within the point group of symmetry at the HF/3-21G(*) level. D_{3h}, C_{2v}, D_3, C_{3v}, and C_s geometries can be depicted as follows (Figure 2). The D_{3h}-symmetric structure possesses all atoms in one plane; rotation of one methylene by 90° gives the C_{2v} structure, and the concerted conrotatory twisting of the three methylene groups leads to the chiral D_3 structure (all four atoms in the SC_3 and SCH_2 groups are coplanar). The C_{3v} structure can be perceived as a product of the 90° rotation of the three methylene groups and subsequent pyramidalization at the central atom, S. Pyramidalization of two methylene groups of the C_{3v} structure and formation of the CC bond between them describes qualitatively the geometry of the C_s structure. The other C_s-symmetric structure (e.g., **2**-C_{s^2}) is similar to the preceding one, but it does not possess the CC bond and the two methylene groups are pyramidalized in the other sense with respect to the third planar methylene group.

The relative energies for **2**-D_3, **2**-D_{3h}, **2**-C_{3v}, **2**-C_s, and **2**-C_{s^2} are similar at the HF/6-31G* level compared to the smaller, 3-21G(*), basis set. Harmonic vibrational frequencies calculated at the HF/6-31G* level reveal a double-well potential energy surface with a D_{3h}-symmetric transition structure for the inversion between two chiral D_3 local minima (Figure 3). The imaginary frequency for **2**-D_{3h} is i467.5 cm^{-1}, and the corresponding real frequency for the conrotatory twisting of the metylene groups in the D_3 structure is 522.2 cm^{-1} (Table II). The barrier for racemization of the D_3 structure, which is 6.4 kcal mol^{-1} at the HF/6-31G* level, rises to 11.4 kcal mol^{-1} after correction for electron correlation at the MP2/6-31G** level, and, finally, it is 9.4 kcal mol^{-1} after ZPVE correction (Tables I and II and Figure 3). The three-membered ring **2**-C_s structure is 55.2 kcal mol^{-1} below the D_3 local minimum and possesses one vibrational normal mode with imaginary frequency, i361.5 cm^{-1}, that corresponds to the pyramidalization of the *exo*-methylene group at the
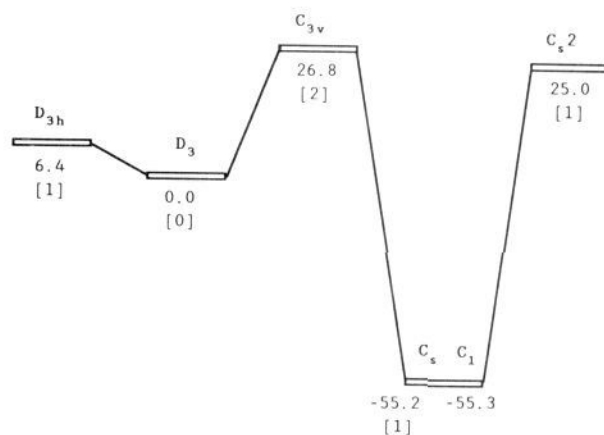

Figure 3. Relative energies (kcal mol^{-1}) for the structures of sulfur trimethylene, $S(CH_2)_3$ (**2**), at the HF/6-31G* potential energy surface. The number of harmonic vibrational frequencies for each structure is given in the square brackets. (The relative energies at the MP level of theory are included in Table I.)

HF/6-31G* level. Thus, we have a double-well PES with **2**-C_s as a transition structure; the minima, which belong to the C_1 point group of symmetry, are only about 0.1 kcal mol^{-1} below **2**-C_s (see Figure 2 and footnote *a* in Table VII). Because of this flatness of the HF/6-31G* PES, the minimum energy structure in this region of the PES may well be (or approximated by) **2**-C_s. Therefore, the MP2/6-31G** energy was calculated for **2**-C_s in order to take advantage of the C_s symmetry. The MP2 result places **2**-C_s 47.7 kcal mol^{-1} below **2**-D_3. Of course, the thietane structure (four-membered ring) is even lower in energy; a single-point HF/6-31G* energy places this structure at least 70 kcal mol^{-1} below **2**-C_s.[19] While **2**-C_s is a transition structure for the inversion at the carbon of the *exo*-methylene group in **2**-C_1, another C_s-symmetric structure (**2**-C_{s^2}) is found to be a transition structure for the process of the circumambulatory scrambling of the carbons at the triple well fragment of the PES with **2**-C_1 as minima (Figure 3). The barrier for the scrambling is 80 kcal mol^{-1}, and the corresponding imaginary frequency is i630.9 cm^{-1} at the HF/6-31G* level.

A question arises about the barrier for the rearrangement of **2**-D_3 to **2**-C_s (**2**-C_1). We cannot locate the relevant transition structure, however. Instead, we identify **2**-C_{3v} as a structure with an imaginary doubly degenerate vibrational mode (i293.9 cm^{-1}) at the C_3- and C_s-symmetric reaction path connecting **2**-D_3 and **2**-C_s (**2**-C_1) (Table II). (**2**-C_{s^2} can also be used as an approximation to the relevant transition structure.) Although **2**-C_{3v} is 26.8 kcal mol^{-1} above **2**-D_3 at the HF/6-31G* level, inclusion of electron correlation (MP2/6-31G**) lowers the relative energy to a mere 0.5 kcal mol^{-1}. This relative energy of 0.5 kcal mol^{-1} is reproduced at the MP2/6-31G* level. Therefore, the smaller 6-31G* basis set was used for the MP3 calculation. The MP3/6-31G* relative energy is 7.7 kcal mol^{-1} and after zero-point vibrational energy (ZPVE) correction is 6.0 kcal mol^{-1}.[20] Because the energy of

(18) Bader, R. F. W. *Pure Appl. Chem.* **1988**, *60*, 145. Bader, R. F. W. *Acc. Chem. Res.* **1975**, *8*, 34; **1985**, *18*, 9. Bader, R. F. W.; MacDougall, P. J. *J. Am. Chem. Soc.* **1985**, *107*, 6788. Bader, R. F. W.; Nguyen-Dang, T. T. *Adv. Quantum Chem.* **1981**, *14*, 63. Bader, R. F. W.; Nguyen-Dang, T T.; Tal, Y. *Rep Prog. Phys.* **1981**, *44*, 893. Bader, R. F. W. *J. Chem. Phys.* **1986**, *85*, 3133.

(19) (a) The HF/6-31G* energy for the thietane, $S(CH_2)_3$, structure is −514.576 54 au at the geometry reported by Brouckere and Broer. See: Brouckere, G.; Broer, R. *Mol. Phys.* **1981**, *43*, 1139. (b) The barrier between **2**-C_s and the thietane structure was not calculated.

(20) (a) For molecules distorted from their equilibrium geometry the restricted MP series tends to exhibit the oscillating behavior such that the MP3 term may even become positive. For example, see: Knowles, P. J.; Somasundram, K.; Handy, N. C.; Hirao, K. *Chem. Phys. Lett.* **1985**, *113*, 8. Consequently, the MP2 energy difference may exceed both the HF and MP3 energy differences between two geometries such as **2**-C_{3v} versus **2**-D_3. The validity of this low-order perturbation correction (MP3) can be questioned, but for these 40-electron molecules more suitable approaches to electron correlation, such as multireference CI, are hardly practical. (b) Recently two MP-based methods for the bond dissociation (RMP4//UMP2) and singlet diradicals (spin-corrected UMP2) have been proposed. See: Gill, P. M. W.; Wong, M. W.; Nobes, R. H.; Radom, L. *Chem. Phys. Lett.* **1988**, *148*, 541. Yamaguchi, K.; Jensen, F.; Dorigo, A.; Houk, K. N. *Chem. Phys. Lett.* **1988**, *149*, 537. Their application to the **2**-D_3/**2**-C_{3v} energy difference would require extensive testing on the ground-state singlets with similar electronic configuration.

Table III. Atomic Charges and the Related Quantities for the Central Atom, X = P, S, and Cl, of the D_3-Symmetric Structures **1**, **2**, and **3**, and the D_{3h}-Symmetric Structures **4**, **5**, and **6**

	1	2	3	4	5	6
Q^a	+3.2	+0.8	−0.5	+4.1	+4.3	+4.0
$\Delta_e{}^{a,b}$	+1.2	−2.2	−4.5	+2.1	+1.3	0.0
$\Delta_r{}^{a,c}$	+2.2	−1.2	−3.5			
$Q(NP)^d$	+1.7	+1.6	+1.4	+2.7	+2.8	+2.7

^{a} Total atomic charge calculated from the total Bader populations (Table IV). ^{b} The difference between the "Q" and the formal charge for the "E" ("no formal double bond") resonance structures. ^{c} The difference between the "Q" and the formal charge for the "R" ("one formal double bond") resonance structures. ^{d} Total atomic charge calculated from the total natural populations (Table VI).
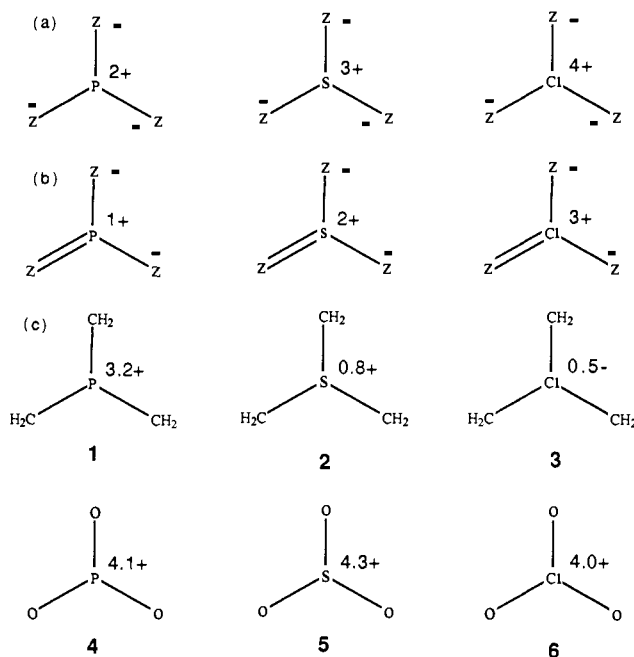
2-C_s is almost identical with that of **2-C_1**, the barrier between **2-D_3** and **2-C_1** should also be a few kilocalories per mole. Thus, experimental detection of **2-D_3** should be possible; resonance-stabilizing substituents at the terminal carbons in a derivative of **2-D_3** (e.g., triphenyl or hexaphenyl) should lower its energy with the respect to **2-C_s** and increase the barrier for the ring closure to **2-C_s** or **2-C_1**.[9b,21] IR and Raman spectra for **2-D_3** and all geometries are available as supplementary material.

P(CH₂)₃⁻ (1) and Cl(CH₂)₃⁺ (3). The PES for **1** has been reported elsewhere and shows qualitative agreement with our results for **2** (Table I).[11] The PES for **3** is dominated by **3-C_s**, which is 90 kcal mol⁻¹ below any other structure at the 3-21G(*) level (Table I). **3-D_3** is 2.0 and 2.6 kcal mol⁻¹ above **3-C_{3v}** at the HF/3-21G(*) and HF/6-31G* levels, respectively. Vibrational frequency calculations indicate that **3-D_3** is a minimum at the PES at the HF/6-31G* level. The mode that corresponds to pyramidalization at Cl with concomitant twisting of the methylene groups ($D_3 \rightarrow C_{3v}$) has a frequency of 85.2 cm⁻¹, that is, much less than 281.1 cm⁻¹ in **2-D_3** even if differences in nuclear masses are taken into account (Table II). Because inclusion of electron correlation is expected to raise **3-D_3** higher above **3-C_{3v}** (if the analogy with **2** holds), **3-D_3** is unlikely to be a local minimum at the PES.

Bonding. The following trends in relative HF/3-21G(*) (or 3-21+G*) energies are observed upon increase in electronegativity of the central atom from P to S and to Cl (Table I): (a) the D_{3h}-symmetric structures are increasingly higher in energy compared with the D_3-symmetric structures; (b) the reverse trend is observed for the three-membered ring C_s-symmetric structures and the C_{3v} structures, which are in the vicinity of the transition structure between D_3 and C_s structures (or C_1); (c) the C_{2v}-symmetric structures, which should roughly approximate barriers for rotation of the single methylene out of resonance, are increasingly higher in energy compared with D_3 structures, but lower compared with D_{3h} structures.

Thus, according to (a), (b), and (c), stabilization gained owing to Y-conjugation decreases in the order of the increasing electronegativity of X (P, S, and Cl); the all-in-plane D_{3h} structures, which are best suited to support large XC π-overlap, are progressively unfavorable. Moreover, if π-overlap were the important factor, the **2-D_{3h}** or, at least, the **2-D_3** should be particularly stabilized because the "X" versus C electronegativity difference is smallest for "X" = S. The relative electronegativities are reflected by the atomic charges obtained from either basis set populations or integration of the electron density within the region around a nucleus confined by the zero-flux surface according to Bader. Bader total atomic charges are compared with the formal π charges for the "no formal double bond" (E) and "one formal double bond" (R) resonance forms. The effects observed are so large that such comparisons between total charges and formal π

Figure 4. Resonance structures ($Z = CH_2$, O) and formal and total atomic charges for the 6π-electron Y-conjugated systems: (a) "E", "no formal double bond" (electrostatic) structures; (b) "R", "one formal double bond" (resonating) structures; (c) total atomic charges (Q) for the central atom calculated from total Bader populations for the Y-conjugated systems (**1–6**) (Tables III and IV).

charges should be qualitatively valid despite polarization of the σ bonds. The calculated charges at the central atom, "X", for **1-D_3**, **2-D_3**, and **3-D_3** are +3.2, +0.8, and −0.5 e, respectively (Figure 4). They exceed charges for the corresponding "E" resonance forms by Δ_e = +1.2, −2.2, and −4.5 e, respectively, and for the "R" forms by Δ_r = +2.2, −1.2, and −3,5 e (Figure 4 and Table III). If π-overlap were important, X(CH₂)₃ with the best match of the atomic charges to its resonating "R" forms would possess the relatively most stable Y-conjugated structure; that is, **2-D_{3h}** (or **2-D_3**) should be especially stabilized because its Δ_r is the smallest, and taking σ polarization into account would make the Δ_r even closer to zero. The unimportance of π-lap is demonstrated by the dependence of the molecular energetics on the relative contribution of "E" versus "R". That is, the more positive Δ_e is, the greater the contribution of "E", and the Y-conjugated structures are more stable. This is, indeed, observed and it means that polarization and electrostatic interactions are responsible for the stabilization that results from π-conjugation.

Properties of the XC bond critical points (BCP), which are the single minima of the electron density along the bond path,[18] confirm the analysis of the atomic charges (Table IV). An increase in electronegativity of "X" from P to Cl shifts the BCP by 0.9 au toward the terminal carbon and increases the electron density (ρ) and ellipticity (ϵ) at the BCP. Therefore, XC overlap is not only larger but also more anisotropic (ϵ), indicating greater π contribution.[22] The Laplacian (∇^2) of the electron density at the BCP achieves a minimum value of −0.517 e (au)⁻⁵ for **2-D_3** (**2-D_{3h}**), that is, indicative of a covalent SC bond and in agreement with the Bader atomic charges.[18] At the same time, the HCXC dihedral angle for the P, S, and Cl D_3-symmetric structures increases (Table IV); clearly, the 3pπ(S)–2pπ(C) π-overlap is unimportant. Polarization functions (d-functions) are large contributors to ϵ in **2-D_3**; e.g., ϵ is 0.279 and 0.674 using 6-31G and 6-31G(2d,p) basis sets, respectively (Table V). This, however, does not indicate that the SC π-overlap possesses a significant 3dπ(S)–2pπ(C), in

(21) Resonance stabilization provided by the aryl groups will be greater for the D_3 structure compared to the C_s or C_1 structure. The ylide-type examples can be provided by the conversion of aziridines to azomethine ylides; the conversion is assisted by the electron-withdrawing and resonance-stabilizing substituents at the terminal carbons. For a review, see: Lown, J. W. *Azomethine Ylides*. In *1,3-Dipolar Cycloaddition Chemistry*; Padwa, A., Ed.; Wiley: New York, 1984; Vol 1, Chapter 6, p 653 (*General Heterocyclic Chemistry Series*; Taylor, E. C., Weissberger, A., Eds.).

(22) Ellipticity (ϵ) is otained according to the following formula: $\epsilon = \lambda^1/\lambda^2 - 1$, where λ^1 and λ^2 are the negative curvatures at the BCP that correspond to the eigenvectors of the Hessian of the electron density perpendicular to the bond path. See: Bader, R. F. W.; Slee, T. S.; Cremer, D.; Kraka, E. *J. Am. Chem. Soc.* **1983**, *105*, 5061.

Table IV. Integrated Bader Atomic Populations (e) for "X", C, and O; Bond Lengths XC and XO (au), and XC (XO) Bond Critical Point Properties; $R(X)$, Distance from X (au); ρ, Electron Density (e (au)$^{-3}$); ϵ, Ellipticity;[22] ∇^2, Laplacian of the Electron Density (e (au)$^{-5}$);[22] HCXC, Dihedral Angle (deg)

		X	C	XC	$R(X)$	ρ	ϵ	∇^2	HCXC
1-$D_3{}^a$	6-31+G*	11.77	7.37	3.161	1.203	0.194	0.529	+0.376	20.3
	3-21+G*	11.69		3.169	1.189	0.191	0.515	+0.750	
1-$D_{3h}{}^a$	3-21+G*	11.67		3.159	1.189	0.192	0.520	+0.735	0.0
2-D_3	6-31G(2d,p)	15.22	6.34	3.029	1.658	0.257	0.674	−0.517	30.1
2-D_{3h}	6-31G*	15.65		3.028	1.845	0.261	0.853	−0.630	0.0
3-D_3	6-31G*	17.51		3.026	2.117	0.247	0.727	−0.282	50.2
		O	XO						
4-D_{3h}	3-21+G*		9.67	2.786	1.128	0.223	0.215	+2.040	
5-D_{3h}	6-31G*	11.72	9.42	2.654	1.037	0.317	0.273	+1.784	
6-D_{3h}	6-31G*		8.97	2.613	1.010	0.405	0.452	+0.407	

^{a} Reference 27.

Table V. SC Bond Critical Points for **2**-D_3 using HF/6-31G* Geometry^a

basis	$R(S)$	λ^1	λ^2	λ^3	ϵ	ρ
6-31G	1.658	−0.328	−0.256	0.194	0.279	0.22194
6-31G*^{b}	1.189	−0.459	−0.253	0.213	0.814	0.27004
	1.317	−0.464	−0.263	−0.105	0.764	0.27045
	1.731	−0.492	−0.290	0.117	0.696	0.26654
6-31G**	1.318	−0.465	−0.265	−0.105	0.756	0.27087
6-31G(2d,p)	1.658	−0.472	−0.282	0.237	0.674	0.25708
6-311G**	1.195	−0.466	−0.260	0.187	0.794	0.27274
	1.297	−0.471	−0.268	−0.111	0.758	0.27299
	1.791	−0.493	−0.287	0.113	0.715	0.26661

^{a} $R(S)$ is distance (au) of the critical point from S. λ^1 and λ^2 (e (au)$^{-5}$) are the eigenvalues of the Hessian of the electron density that correspond to eigenvectors perpendicular to the SC bond path (SC bond axis here); λ^3 is related to the third component that is along the bond path. ϵ is defined in ref 22. ^{b} Integrated electron populations for S are 13.55, 14.22, and 15.46 for the $R(S)$ = 1.189, 1.317, and 1.731 au critical points, respectively; thus, each of the three pseudoatoms possesses 0.7 electron.

Table VI. Natural Populations (NP) and Natural Atomic Orbital (NAO) Populations for the D_{3h}-Symmetric Structures XZ$_3$ (X = P (anion), S (neutral), Cl (cation), and Z = C, O) at the HF/3-21+G* for **1** and **4**, and HF/6-31G* for the Other Structures

	total NP		NAO population	
	X	Z	3pπ(X)	2pπ(Z)
1^a	13.30	7.35	0.88	1.69
2	14.43	7.04	1.21	1.56
3	15.60	6.73	1.56	1.44
4^a	12.30	9.23	0.56	1.79
5	13.22	8.93	0.82	1.69
6	14.30	8.57	1.14	1.57

^{a} Reference 14.

addition to 3pπ(S)–2pπ(C), component because similar (though smaller magnitude changes of ϵ as a function of the basis have been found for the CC bond in ethylene.[27] (3dπ(X)–2pπ(C) overlap cannot create a barrier for rotation about the XC bond.)

Surprisingly, the HF/6-31G* electron density indicates the presence of a local maximum flanked by two minima along the SC bond path (and the SC bond axis) in **2**-D_3 (Table V). Such maxima, "pseudoatoms", have been recently reported in lithium and sodium clusters, and their presence has been interpreted as indication of an onset of metallic character.[23] Otherwise, an approach to a zero band gap in a metal corresponds to a small HOMO–LUMO energy gap in a cluster or molecule; a smaller HOMO–LUMO energy gap, however, indicates a weak bond. (CS)$_n$ hexagonal sheet polymer,[24] may not be metallic, but, undoubtedly, π-bonding in **2**-D_3 is very weak despite a large π-overlap. The "pseudoatom" in **2**-D_3 possesses 0.7 e. The electron density differences between the maximum and the minima are on the order of 1% of the electron density at the maximum. The eigenvalue of the Hessian of the electron density (λ^3) that corresponds to the eigenvector directed along the SC bond axis (curvature of the electron density in this direction) is only −0.1 e (au)$^{-5}$ at the "pseudoatom" (Table V). In fact, it is more appropriate to view the electron density at the SC bond path as very flat (small curvature along the SC bond axis) within the middle 1-au long segment.

Addition of polarization functions at the hydrogens or the third sp-valence shell (s at the hydrogens) has little effect on the electron densities; that is, the HF/6-31G** and HF/6-311G** electron densities are very similar to the discussed HF/6-31G* density and, in particular, they possess "pseudoatoms". Removal of the d-

functions (6-31G) or use of the two sets of the d-functions, which are effectively equivalent to one set of d-functions with an optimized d-exponent, at both S and C (6-31G(2d,p) gives a single SC bond critical point (Table V). Thus, one of the origins of the "pseudoatoms" can be an unoptimized exponent of the d-functions of 6-31G*, 6-31G**, and 6-311G** basis sets.[25a] Moreover, the restricted HF/6-31G* wave function for **2**-D_3 is on the verge of the symmetry breaking (UHF instability).[25b] Both balanced electron correlation correction and more complete basis set may qualitatively change the bond path in its region of flatness.[25]

If our assertion about the preponderance of the "no formal double bond" (E) resonance form is valid, replacement of the terminal methylene groups with the isoelectronic but more electronegative oxo groups should aid Y-conjugation. Indeed, all oxides **4**, **5**, and **6** are D_{3h}-symmetric species. In the case of ClO$_3{}^+$ another pyramidal C_{3v}-symmetric structure (**6**-C_{3v}) is found 90.8 kcal mol^{-1} above **6**-D_{3h} at the HF/6-31G* level (Table VII). The analogous energy difference **3**-C_{3v} versus **3**-D_3 is −2.6 kcal mol^{-1} (Table I). Atomic charges derived from Bader atomic populations are approximately constant and equal to +4 at the central atom for all three oxides that should be compared to the sharp decrease of the central atom charge by 3.7 e in **1**-D_3 versus **3**-D_3 (Table III and Figure 4). This is the consequence of the greater electronegativity of O versus C; that is, the oxides are highly ionic. Although the response of the atomic charges in oxides to the variation of the electronegativity of "X" is smaller than their carbon counterparts, an increase in electron density (ρ) and the

(23) Cao, W. L.; Gatti, C.; MacDougall, P. J.; Bader, R. F. W. *Chem. Phys. Lett.* **1987**, *141*, 380. Gatti, C.; Fantucci, P.; Pacchioni, G. *Theor. Chem. Acta* **1987**, *72*, 433.

(24) For a review on carbon monosulfide, see: Moltzen, E. K.; Klabunde, K. J.; Senning, A. *Chem. Rev.* **1988**, *88*, 391.

(25) (a) Distance dependence of one of the Cartesian components of the basis d-function, e.g., d$_{x^2}$, is that of a Gaussian multiplied by x^2. Therefore, the electron density described by d-functions tend to be relatively significant further from the center nucleus compared to the density that originates from p- or s-functions. Single sets of d-functions with an unoptimized electron density in the internuclear region and, therefore, for weak bonds with flat electron density a spurious local maximum (pseudoatom) is probable. (b) Stability testing of the restricted HF/6-31G* wave function for **2**-D_3 with the respect to the UHF wave function using standard options of GAUSSIAN 82 program gives the lowest root of +0.0064 only. (c) In terms of the reference MO's (e.g., in CI), inclusion of electron correlation corresponds to population of the antibonding MO's. Therefore, correlated wave function would generally show depletion of the electron density in the internuclear region, and formation of "pseudoatoms" is less probable for correlated electron densities. In relation to ref 23 we note that the RHF/6-31G(2d) wave function for Li$_2$ (Li–Li distance is 5.10 au) is UHF unstable (one negative root of −0.0138).

Table VII. Total Energies (-au)[a]

		D_3	D_{3h}	C_{2v}	C_{3v}	C_s	C_s^2
2	3-21G(*)	511.884 73	511.874 26	511.859 28	511.837 01	511.959 09	511.8387
2	6-31G*	514.362 44	514.252 20		514.319 68	514.450 33[b]	514.3225
2	6-31G**[c]	514.374 72	514.364 73		514.331 10	514.461 37	
	MP2/6-31G**[c]	514.947 81	514.929 59		514.946 98	515.023 79	
	MP2/6-31G*[c]	514.898 20			514.897 40		
	MP3/6-31G*[c]	514.926 70			514.914 35		
3	3-21G(*)	573.129 23	573.090 26	573.091 94	573.132 47	573.276 10	
3	6-31G*	575.859 77	575.822 00		575.863 84		
5	6-31G*		621.981 57				
6	6-31G*		683.233 34		683.091 80		

[a] The HF/6-31G* optimized geometries are available as supplementary material. [b] Full C_1 geometry optimization causes pyramidalization of the exo carbon; the energy is: -514.450 55. [c] At the HF/6-31G* optimized geometry.

elliticity (ϵ) at the XO BCP are still significant. Similarly, Laplacian (∇^2) at the BCP is also very sensitive to change in the electronegativity of "X", and its large positive values indicate high ionicity of the XO bonds (Table IV).[18]

6-C_{3v} possesses a geometry similar to that of the chlorate anion, ClO_3^-;[26] this raises a possibility of detection of **6**-C_{3v} as an intermediate in two-electron oxidation (or detachment in the gas phase) of ClO_3^-. Of course, knowledge of the barrier for planarization (which probably is miniscule) to **6**-D_{3h} and PES for ClO_3 radical would be helpful.

Natural populations (NP) predict much less ionic bonds compared with the results from Bader atomic populations, but, nevertheless, they reproduce qualitatively trends pertinent to the Bader atomic populations. Atomic charges at "X" = P, S, Cl for the Y-conjugated X(CH₂)₃ calculated from Bader atomic populations and total NP (Table VI) are +3.2, +0.8, -0.5 and +1.7, +1.6, +1.4 e, respectively (Table III). Analogous results for the oxides, XO₃ are +4.1, +4.3, +4.0 and +2.7, +2.8, +2.7 e, respectively (Figure 4 and Table III). Enhanced charge transfer to "X" for "X" = P, S, Cl is reflected in NAO populations for the 3pπ(X) orbitals: 0.88, 1.21, 1.56 and 0.56, 0.82, 1.14 e for **1**-D_{3h}, **2**-D_{3h}, **3**-D_{3h}, and **4**-D_{3h}, **5**-D_{3h}, **6**-D_{3h}, respectively (Table VI). Because NAO populations tend to exaggerate the 3pπ orbital contribution to the bonding π-MO,[14] the NAO populations in **2**-D_{3h} and **6**-D_{3h} are closest to unity; an ideal Hückel 6π-electron Y-conjugated system has a π population of one electron at the central atom. Therefore, in agreement with conclusions drawn from the topological analysis of the total electron density, Y-conjugated **2** possesses the greatest π-overlap compared to **1** and **3**.

Pauling,[28] who introduced electronegativity a half of century ago, pointed out that the bond energy between unlike atoms is usually greater than the average of the bond energies for the corresponding homoatomic bonds. These energy differences were used to define the electronegativity scale. The contribution of

the ionic resonance form was related to the greater bond energy for the heteroatomic bonds. Our results imply that even *small* electronegativity difference between the multiply bonded atoms in the conjugated system may lead to the dominant contribution of the fully ionic resonance form, e.g., in P(CH₂)₃⁻, and significant stabilization of the conjugated system (vide Conclusions). Although these empirical ideas once linked to electronegativity are supplanted by more rigorous theoretical approaches,[29] electronegativity in its simplest form is still useful and an important concept in bonding.

Conclusions

Multiple bonds between first- and second-row elements have an electrostatic nature; π-overlap is unimportant. The stablity of such π-conjugated systems is increased the more the relative electronegativities (and atomic charges) conform to formal atomic charges in "no formal double bond" resonance form.

Preparation of the Y-conjugated S(CH₂)₃ (or its derivative) is feasible. (CS)ₙ polymers may have interesting electronic properties; their characterization is highly recommended.[24]

Supplementary Material Available: Listing of IR and Raman spectra for **2**-D_3 and all geometries for **2**, **3**, **5**, and **6** (12 pages). Ordering information is given on any current masthead page.

(26) Francisco, J. S.; Williams, I. H. *Chem. Phys. Lett.* **1987**, *114*, 339 and references therein.
(27) Rajca, A., manuscript in preparation.
(28) Pauling, L. *The Nature of the Chemical Bond*, 3rd ed.; Cornell University Press, New York, 1960.

(29) Boyd, R. J.; Edgecombe, K. E. *J. Am. Chem. Soc.* **1988**, *110*, 4182. For a review on electronegativity, see: Electronegativity In *Structure and Bonding*; Sen, K. D., Jorgensen, C. K., Eds.; Springer-Verlag: Berlin, 1987; Vol 66.